Estimation of atmospheric CO_2 concentrations through the data assimilation of AIRS radiances in the ECMWF 4D-Var system

Richard J. Engelen

European Centre for Medium-Range Weather Forecasts, Shinfield Park, Reading, RG2 9AX, UK.
(richard.engelen@ecmwf.int)

ABSTRACT

Atmospheric CO_2 concentrations have been obtained from AIRS radiance data within the ECMWF data assimilation system. A subset of channels from the AIRS instrument on board the NASA Aqua platform has been assimilated providing estimates of tropospheric and stratospheric column-average CO_2 mixing ratios. Although global estimates are obtained, the information content of the tropospheric estimates at mid- and high-latitudes is limited, and results are therefore only presented for the tropical region. First results for April 2003 show considerable geographical variability compared to the background with values ranging between 372 and 383 ppmv. These CO_2 values are representative for a layer between the tropopause and about 600 hPa. The monthly mean random error is about 1 %. Careful error analysis has been carried out to minimize any systematic errors. This study has demonstrated the feasibility of global CO_2 estimation using AIRS data in an NWP data assimilation system. In the future the system will be improved to treat CO_2 as a full 3-dimensional atmospheric variable, including transport.

1 Introduction

The importance of accurate observations of atmospheric CO_2 for top-down estimates of carbon sources and sinks has been recognized for almost a decade. In this period various synthesis inversion studies have been carried out using surface flask observations of CO_2 concentrations to estimate carbon sources and sinks at the Earth's surface [Enting et al. (1995); Fan et al. (1998); Rayner et al. (1999); Bousquet et al. (1999a,b); Kaminski et al. (1999); Peylin et al. (2000); Gurney et al. (2002)]. These flask measurements are highly accurate, but are limited to less than 100 sites globally. This makes the inversion problem highly data limited, especially in the tropics, where there are few surface flask stations. For some years now there has been a growing interest in the use of satellite data to improve estimates of the spatial and temporal variability of atmospheric CO_2. In particular, the development of a new generation high-spectral resolution sounders that observe the atmosphere in the infrared and/or the near-infrared triggered several studies on the capabilities of these instruments to provide information on atmospheric CO_2. Rayner and O'Brien (2001) showed that these satellite observations have the potential to improve current CO_2 inversions, if the accuracy of their monthly mean values is better than 2.5 ppmv. Engelen et al. (2001a) performed a simulation study to look at the capabilities of the Atmospheric Infrared Sounder (AIRS), Chédin et al. (2003) did similar simulations for the Infrared Atmospheric Sounding Interferometer (IASI), and O'Brien and Rayner (2002) studied the near-infrared option, which might be realised by the Orbiting Carbon Observatory (OCO) mission. However, so far there is only one study that has been performed with real satellite data; Chédin et al. (2002) used data from the Tiros Operational Vertical Sounder (TOVS) to infer atmospheric CO_2 concentrations in the tropics. Although the capabilities of the TOVS instrument are limited with respect to CO_2 [Engelen and Stephens (2004)], the results of Chédin et al. (2002) are promising.

Data from the AIRS instrument have been assimilated operationally in the European Centre for Medium-Range Weather Forecasts (ECMWF) four-dimensional variational (4D-Var) data assimilation system since October
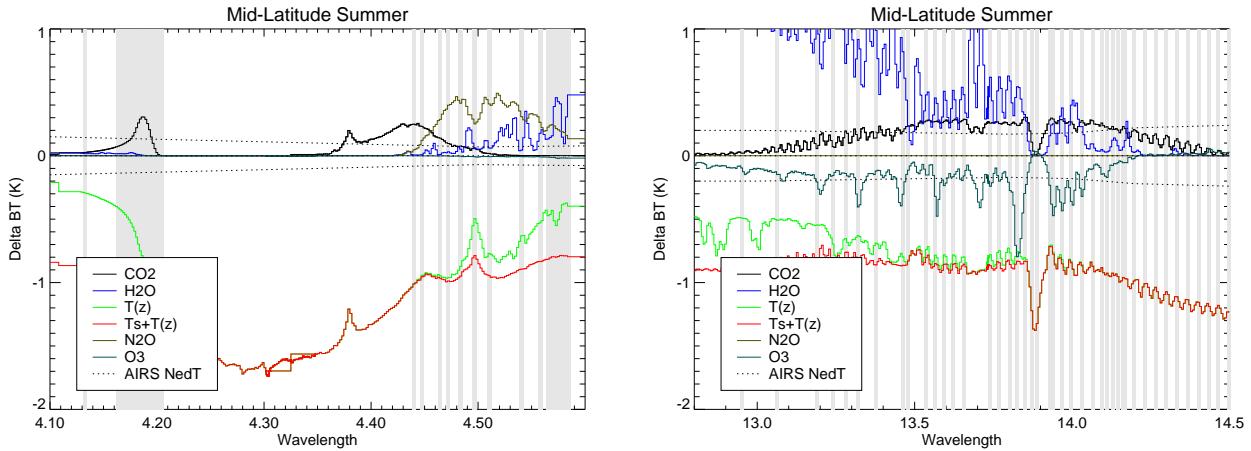
Figure 1: Nice Figure.

2003 [McNally et al., this volume]. Although the main purpose of this assimilation is to improve the temperature, water vapour, and ozone fields as well as the dynamics, efforts are being made to also extract other information from the observed radiances. Figure 1 shows the sensitivity of the observed radiances to changes in several atmospheric variables for the short-wave and long-wave CO$_2$ bands. Strong responses exist for atmospheric temperature, surface temperature, and water vapour. The figure also shows CO$_2$ sensitivity, although it is much weaker than the other signals. However, the spectral correlation of an specific gas absorption line distribution will also help to distinguish between the various variables. Therefore, it is feasible to extract information about CO$_2$ from the observed radiances and a column CO$_2$ estimation has been implemented in the data assimilation system as described in this paper. Whilst having more realistic CO$_2$ concentrations in the forecast model could in principal be beneficial for the short-term weather forecast [Engelen et al. (2001b)], this in itself was not the main purpose of this research. The aim is to produce global CO$_2$ fields from the AIRS satellite data with accuracy high enough for carbon flux inversions. It is therefore important to have an accurate characterisation of the CO$_2$ estimates including their errors.

The main benefit of estimating CO$_2$ mixing ratios within a numerical weather prediction (NWP) data assimilation system is that temperature and humidity, which also affect the observed infrared radiances are well constrained by various other measurements and by the forecast model itself. For example, ECMWF assimilates radiances from three Advanced Microwave Sounding Unit A (AMSU-A) instruments, three Special Sensor Microwave Imager (SSM/I) instruments, two AMSU-B instruments, five geostationary satellites, two High Resolution Infrared Radiation Sounder (HIRS) instruments, and many radiosondes and aircraft constraining both temperature and water vapour on smaller vertical scales. These additional observational constraints on temperature and water vapour assist the extraction of atmospheric CO$_2$ from the AIRS observations within the NWP system.

2 Set-up of the CO$_2$ data assimilation system

2.1 CO$_2$ as a column variable

Within the 4D-Var system CO$_2$ is currently estimated as an independent column variable. This means that CO$_2$ is not a tracer variable in the transport model and is estimated only at the observation locations. Background error correlations between CO$_2$ and the other assimilation variables are neglected. In practice this means that, while the forecast model variables (e.g., temperature and water vapour) appear in the control vector ($\delta\mathbf{x}(t_0)$)

as 3-dimensional fields, CO_2 appears as a vector of column variables at the observation locations. The link between the initial state and the states at observation locations and times is absent for CO_2. Another important difference between the CO_2 variable and the regular analysis variables (temperature, water vapour, etc.) is that the background field of the regular variables is based on a forecast that uses the previous analysis as its initial state. For CO_2, each analysis uses a climatological background state of CO_2. CO_2 information is thus not carried over from one analysis to the next.

This methodology was used as a first step to implement CO_2 in the data assimilation system making use of the current operational architecture. It makes full use of the accurate temperature and water vapour analysis fields constrained by all available observations, but there are also some limitations. Firstly, the individual CO_2 estimates are not constrained by the model transport during the 12-hour assimilation window. During this 12-hour time span the model transport is usually accurate and can help to advect information from one place to another. Secondly, by assimilating column CO_2 values instead of full profiles a hard constraint is applied to the analysis in the form of a fixed profile shape. This removes some of the flexibility in the adjustments and can lead to errors if the used profile shape is far from the truth. This hard constraint also means that all vertical levels are fully correlated and any adjustments in the stratosphere will therefore also adjust the troposphere. In case of many stratospheric radiance channels and only few tropospheric radiance channels this leads to a dominant stratospheric signal in the estimated CO_2 column value.

Based on first results (not shown here) indicating that the column variable was indeed dominated by the large amount of stratospheric AIRS channels, the column variable was split into a tropospheric column and a stratospheric column. These two columns act as independent variables without any error correlation in the analysis. The tropopause height that separates the two columns, is estimated from the background temperature profile using an algorithm based on lapse rates, and varies with location. This ensured that the tropospheric analysis results were not dominated by the stratosphere. However, any potentially useful correlations between stratospheric CO_2 and tropospheric CO_2 are disregarded. The tropospheric column can be quite variable in the vertical. Depending on the tropopause height and the cloud top height, the column varies from shallow to deep allowing respectively less or more channels to be used in the tropospheric analysis.

As described in McNally and Watts (2003), the cloud detection algorithm searches for channels that are unaffected by clouds within the error margin of the observations and radiative transfer modelling. Within the algorithm the channels are ranked in vertical space by assigning them a "trip" level that represents the height of an opaque cloud needed to affect the specific channel by more than 1%. The 1% number is somewhat arbitrary, but is only used to rank the channels; it does not represent any error treshold in the remaining channel radiances. After the cloud detection the lowest trip level of the remaining channels then approximates the lowest level of the observation sensitivity. If there is a cloud, this corresponds to the cloud top height; if there is no cloud, it corresponds to the lowest level of the clear column where the observation is still sensitive to CO_2. Areas with consistent high cloud cover will therefore affect the thickness of the tropospheric estimated CO_2 column.

2.2 Analysis error estimation

It is crucial to have an estimate of the individual analysis errors to properly interpret the analysis results. Initially, the analysis error (σ_a) within the 4D-Var system was calculated from the background error (σ_b), the observation error covariance ($\mathbf{R}$), and the CO_2 Jacobians ($\mathbf{H}$):

$$\sigma_a^2 = [\sigma_b^{-2} + \mathbf{H}^T \mathbf{R}^{-1} \mathbf{H}]^{-1} \tag{1}$$

The errors in the temperature, water vapour, and ozone profiles that enter the radiative transfer equation are taken into account by inflating the observation error covariance ($\mathbf{R}$) based on the sensitivity of the radiative

transfer to perturbations defined by the respective background covariance matrices. Although this is a simplification of the real error model, it is sufficient for our purposes. Besides, the CO$_2$ analysis itself is part of a multivariate minimization problem that takes into account all relevant error sources.

Within a variational assimilation system the equation above requires separate calculations of the Jacobians **H** for each observation, which amounts to significant extra computer time. Because the analysis error is in first approximation a function of the tropospheric temperature lapse rate and the number of assimilated AIRS channels peaking in the troposphere (determined by the tropopause height and the cloud top height), a non-linear regression (artificial neural network [e.g., Rumelhart et al. (1986)]) was used to relate the analysis error to these two variables. The neural network was trained with data from March 2003 and then used to estimate the analysis errors for all other months.

3   Results

Some first results of the CO$_2$ data assimilation scheme are presented here to illustrate the capabilities of the system. The tropospheric background values used in the assimilation, shown in Figure 3, were zonal mean monthly averaged mixing ratios based on surface flask observations from the previous year [GLOBALVIEW-CO$_2$ (2003)]. These averaged flask observations are based on maritime air samples and a constant value of 2 ppmv was added to compensate for the annual trend. For the stratospheric background a constant value of 375 ppmv was used. The background error was set to 30 ppmv and was deliberately taken large to minimise the contribution of the background to the analysis in these preliminary experiments. Individual analysis values at the observation locations were gridded onto a 1 x 1 latitude-longitude grid for a whole month. Within a grid box the data were averaged using a weighted average with the analysis errors as weights. This 1 x 1 grid was then smoothed with a 15 x 15 moving boxcar average. Each individual grid box needed to have more than 10 observations within a month to be included in the smoothing averaging. Therefore, some geographical areas have no data in the final monthly mean fields because of consistent high cloud cover.

3.1   Quality of analysis

The information content of the CO$_2$ estimates is highly variable due to variations in temperature lapse rate and cloudiness (see also section 2.2) and, therefore, the contribution of the background to the analysis estimate varies as well. The value of the analysis error relative to the background error shows how much information is gained from the observations and can be formally represented by the averaging kernel [Rodgers (2000)], which is for a single scalar analysis variable defined as:

$$A = 1 - \frac{\sigma_a^2}{\sigma_b^2} \tag{2}$$

The averaging kernel varies between 0 and 1, where 0 means that we retrieve the background value back in the analysis, while 1 means that we have an analysis independent of the used background. With a constant background error (as currently used) there is no fundamental difference between the averaging kernel and the analysis error itself, but when the background error varies geographically, the averaging kernel is much easier to interpret. Also, the absolute values of the averaging kernel largely depend on the value of the background error. We will therefore only use the relative values of the averaging kernel, because our assumption of a very large background error causes the averaging kernel to be unrealistically close to one. Figure 2 shows the mean averaging kernel for April 2003 using all available channels on teh left and using clear field-of-views only on the right. It is immediately clear that the information content of the analysis is highest in the tropics, but degrades quickly at higher latitudes. This is caused by the shallower troposphere (lower tropopause) and the
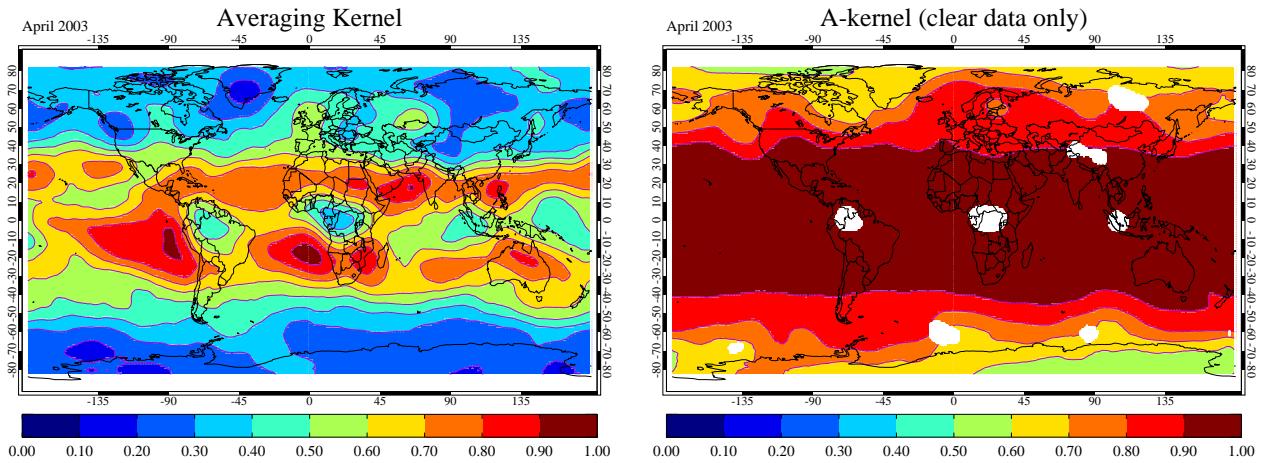
Figure 2: Averaging kernel averaged for April 2003 on a 1 x 1 grid using all available channels (left) and using clear field-of-views only (right).
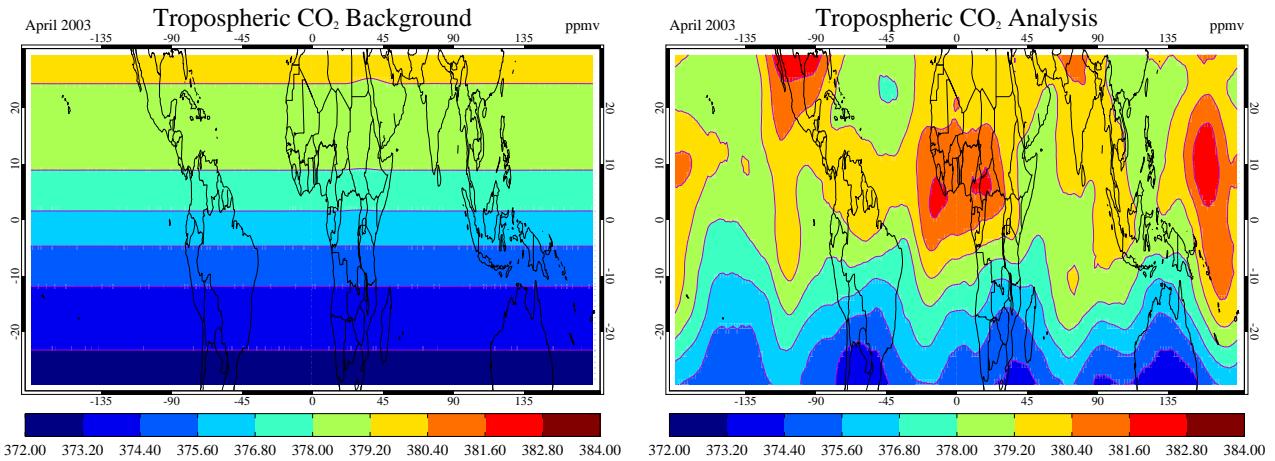
Figure 3: Background (left) and analysis (right) CO$_2$ distribution averaged for April 2003.

smaller temperature lapse rate at higher latitudes. Also, tropical convective areas have a much smaller mean averaging kernel value due to high cloud top levels. However, in these cloudy tropical areas there are still many occasions where the satellite instrument sees clear areas or areas with low clouds, even in the convective regions. This is shown by the clear fov plot on the right that shows a homogeneous averaging kernel field throughout the tropical area. Therefore, it is still possible to calculate monthly mean CO$_2$ concentrations for most of these areas. Based on Figure 2 we will show only analysis results for the region between 30 S and 30 N. CO$_2$ is estimated outside this region, but the results depend significantly on the assumed background values.

3.2 Monthly mean CO$_2$ distribution

Figure 3 shows the CO$_2$ analysis results for April 2003. The left panel shows the background values and the right panel shows the actual analysis results. The background field is not entirely zonal, because the individual observations are not homogeneously distributerd over the averaging grid and each individual background value was interpolated in latitude from the GlobalView zonal means. The figure shows that the analysis adds struc-

ture to the zonal background field. Although the main north-south gradient remains, meridional variability is produced by the analysis. In the equatorial region the analysis tends to have more CO$_2$ in the convective areas, especially in the West Pacific. Another feature can be observed over the southern part of North America. A careful analysis was done using AMSU-A data to see if these features were caused by biases in the temperature analysis. This seems indeed to be the case for the high values over southern North America in April, where a cold bias is observed in the temperature analysis field compared to AMSU-A measurements. This could cause a positive bias in the CO$_2$ field. However, for the other regions such a cold analysis bias is not present. Also, plots of AIRS first-guess departures (the difference between the observed brightness temperatures and the model simulated brightness temperatures from the 6-hour forecast) that drive the analysis show the same patterns as the CO$_2$ analysis field. These patterns are very dissimilar from the AMSU-A first-guess departures and can therefore not be explained completely by errors in the temperature forecast. To further illustrate
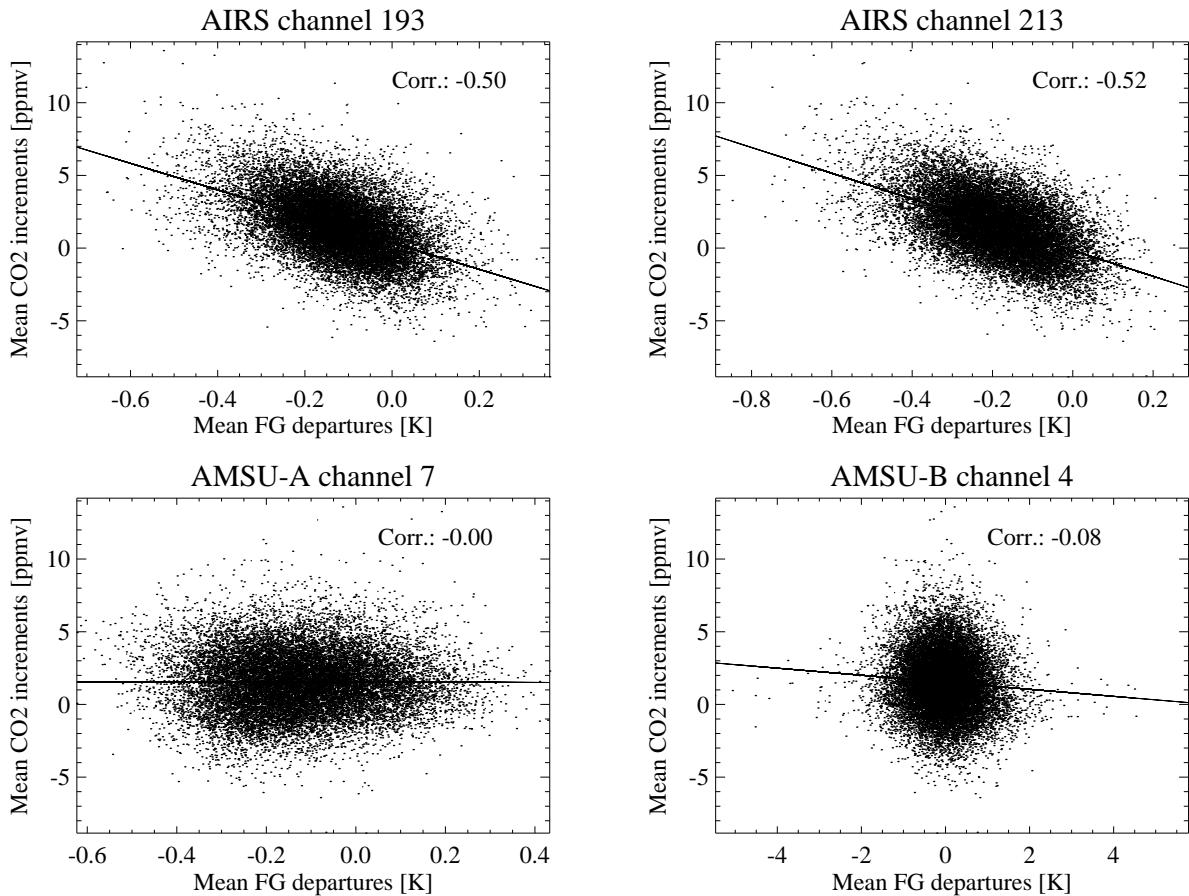
Figure 4: Monthly mean CO$_2$ increments as a function of observation departures for AIRS channels 193 and 213, AMSU-A channel 7, and AMSU-B channel 4.

the point, we have plotted in Figure 4 the monthly mean CO$_2$ increments (analysis minus background) as a function of the observations departures for AIRS channels 193 and 213 (both sensitive to mid-tropospheric CO$_2$), AMSU-A channel 7 (sensitive to mid-tropospheric temperature), and AMSU-B channel 4 (sensitive to tropospheric water vapour). Any biases in the model temperature and water vapour fields that are aliased in the CO$_2$ results would show up as correlations in the 2 AMSU plots. While there is a significant correlation in the two AIRS plots, such correlations are not shown in the AMSU plots. Although these results are not conclusive, they indicate that the effect of model temperature and water vapour biases on the CO$_2$ analysis is not large.

118
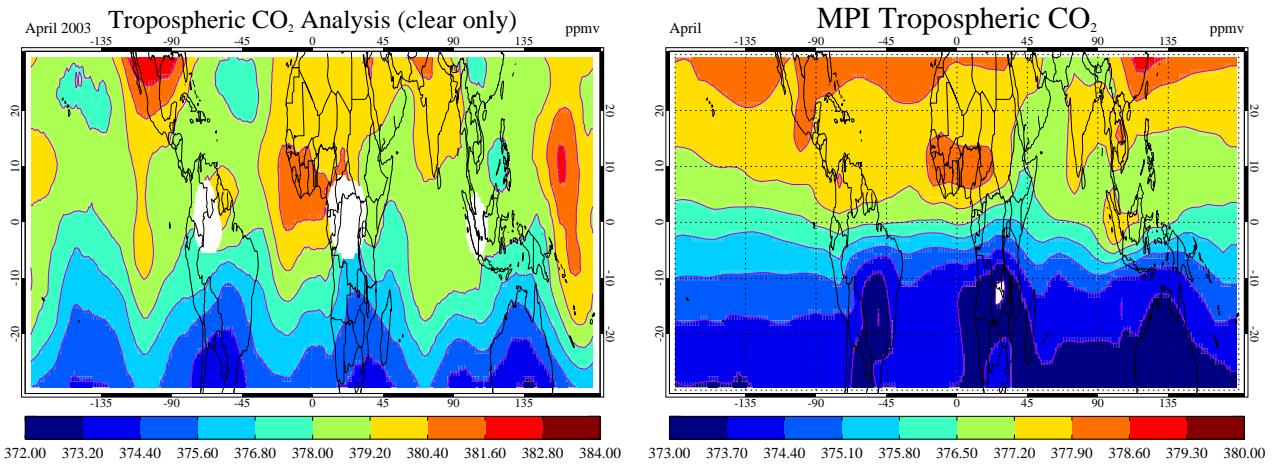
Figure 5: CO$_2$ analysis distribution averaged for April 2003 using clear field-of-views only (left) and model simulation of tropospheric CO$_2$ for the same period from the Max Planck Institute for Biogeochemistry (right).

The higher CO$_2$ values on the westside of Africa in April could be explained by biomass burning effects. Similar patterns in the MOPITT carbon monoxide observations can be observed over that area in April 2003 (see http://www.eos.ucar.edu/mopitt/data/index.html). The high values in the western Pacific are probably more surprising. One explanation could be that anthropogenic emissions from south-east Asia are lifted up and transported to the western Pacific by the general circulation. During this part of the year there is a circular wind pattern in the middle troposphere bringing air east from the south-east Asian coast and then south to the middle of the Pacific. However, more careful analysis of the results should be carried out before drawing firm conclusions. For example, clouds are detected in our cloud detection scheme within a small error margin. Therefore, it is in principle possible to have a systematic error in the lower channels due to undetected clouds resulting in a CO$_2$ bias of a few ppmv. Also, air-mass dependent errors in the radiative transfer (e.g., the spectroscopy) could cause systematic errors in the CO$_2$ analysis results on regional scales.

Although it is possible to have an estimate of CO$_2$ in the convective areas, the layer represented by this estimate is much shallower than in areas with low clouds or no clouds at all. This could in principle make results harder to interpret. When only cloud-free fovs are used, the thickness of the column if more uniform. For comparison, the left panel of Figure 5 shows the CO$_2$ analysis results for April 2003 using clear fovs only. The CO$_2$ values are slightly lower than the values shown in Figure 3, but the geographical patterns remain very similar. However, if the thickness of the representative layer as well as the estimated analysis error are taken into account, using all available data has the advantage of better spatial and temporal cover. This could be a significant benefit in surface flux inversion studies. For comparison, Figure 5 also shows a model simulation for the same period with the TM3 model from the Max Planck Institute for Biogeochemistry in Jena (Y. Tiwari, personal communication, 2004). Although the amplitude of the gradients is smaller in the model simulations (notice different colour scale), patterns are quite similar. The model tends to generate a more zonal distribution but the high values over West Africa and the lower values along the East-African coast are similar. the main difference is probably the high values over the Western Pacific that are missing in the model simulations.

3.3   Error estimate

To provide an indication of the error in the monthly mean CO$_2$ distribution Figure 6 shows the individual analysis errors averaged under different assumptions. The minimum error is calculated assuming that the
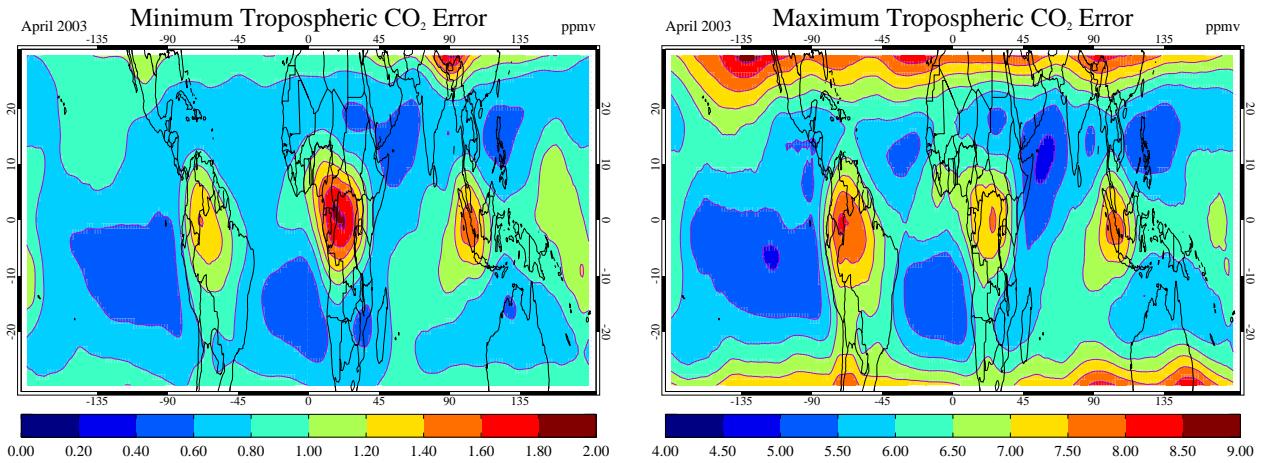
Figure 6: Lower (left) and upper (right) estimate of the error in the monthly averaged CO$_2$ distribution for April 2003.

errors of all individual estimates are completely uncorrelated using the following equation:

$$\overline{\sigma}_{\min} = \left(\sum_i^N \frac{1}{\sigma_i^2} \right)^{-1/2} \tag{3}$$

which implies a $\sqrt{N}$ reduction of the individual errors. The maximum error is calculated assuming that the errors of all individual estimates are correlated using the following equation:

$$\overline{\sigma}_{\max} = \frac{1}{N} \sum_i^N \sigma_i \tag{4}$$

Both error estimates clearly depend on the number of observations in the monthly average with cloudy areas having larger errors. Neither error estimate includes systematic errors, but their range gives a reasonable estimate of the average random error. For the tropical area the expected monthly-average analysis error is therefore between 1 and 6 ppmv, which is on the order of 1%.

4   Summary

Global estimates of CO$_2$ concentrations have been obtained from AIRS radiance data. A subset of channels from the AIRS instrument on board the NASA Aqua platform has been assimilated in the ECMWF data assimilation system providing estimates of tropospheric and stratospheric CO$_2$ mixing ratios. Currently, CO$_2$ is not included as a tracer in the transport model, but treated as a column variable estimated at the time and location of each AIRS observation entering the sytem. This setup has enabled first CO$_2$ assimilation experiments, but has the disadvantage that it lacks the transport constraint and the adjustment flexibility in the vertical. The analysis errors have been estimated using a artificial neural network that relates the CO$_2$ analysis error to the number of assimilated channels sensitive to tropospheric CO$_2$ and the tropospheric temperature lapse rate based on earlier simulations that estimated the analysis error using Bayesian theory.

First results for April 2003 are presented showing considerable geographical variability compared to the background. Various quality checks were carried out to exclude as many potential error sources as possible. Careful analysis is needed to guarantee the validity of results considering the small CO$_2$ signal compared to these various error sources. Although the results presented in this paper have been quality-checked, more error analysis and validation will be carried out in the near future.

The current results show CO$_2$ values ranging between 372 ppmv and 383 ppmv in the tropics with an estimated error of about 3 ppmv for the monthly average. These values are representative for a layer between the tropopause and about 650 hPa if only observations from cloud-free field-of-views are used. The lower boundary of the representative layer varies between 500 and 700 hPa, when also observations are used where some channels have been removed by the cloud detection algorithm.

This study has demonstrated the feasibility of global CO$_2$ estimation using AIRS data in an NWP data assimilation system. In the future the system will be improved to treat CO$_2$ as a full 3-dimensional atmospheric variable, including transport.

Acknowledgments

References

Aumann, H. H., M. T. Chahine, C. Gautier, M. D. Goldberg, E. Kalnay, L. M. McMillin, H. Revercomb, P. W. Rosenkranz, W. L. Smith, D. H. Staelin, L. L. Strow, and J. Susskind, 2003: AIRS/AMSU/HSB on the Aqua mission: design, science objectives, data products, and processing systems. *IEEE Trans. Geosci. Remote Sensing*, **41**, 253–264.

Bousquet, P., P. Ciais, P. Peylin, M. Ramonet, and P. Monfray, 1999a: Inverse modeling of annual atmospheric CO$_2$ sources and sinks, 1, Method and control inversion. *J. Geophys. Res.*, **104**, 26161–26178.

Bousquet, P., P. Ciais, P. Peylin, M. Ramonet, and P. Monfray, 1999b: Inverse modeling of annual atmospheric CO$_2$ sources and sinks, 2, Sensitivity study. *J. Geophys. Res.*, **104**, 26179–26194.

Chédin, A., A. Hollingsworth, N. A. Scott, S. Serrar, C. Crevoisier, and R. Armante, 2002: Annual and seasonal variations of atmospheric CO$_2$, N$_2$O and CO concentrations retrieved from NOAA/TOVS satellite observations. *Geophys. Res. Let.*, **29**(8).

Chédin, A., R. Saunders, A. Hollingsworth, N. Scott, M. Matricardi, J. Etcheto, C. Clerbaux, R. Armante, and C. Crevoisier, 2003: The feasibility of monitoring co$_2$ from high-resolution infrared sounders. *J. Geophys. Res.*, **108**(D2).

Courtier, P., J.-N. Thépaut, and A. Hollingsworth, 1994: A strategy for operational implementation of 4D-Var, using an incremental approach. *Q. J. R. Met. Soc.*, **120**, 1367–1387.

Crevoisier, C., A. Chedin, and N. A. Scott, 2003: AIRS channel selection for CO$_2$ and other trace-gas retrievals. *Q. J. R. Met. Soc.*, **129**, 2719–2740.

Engelen, R. J., A. S. Denning, K. R. Gurney, and G. L. Stephens, 2001a: Global observations of the carbon budget 1. Expected satellite capabilities for emission spectroscopy in the EOS and NPOESS eras. *J. Geophys. Res.*, **106**, 20055–20068.

Engelen, R. J. and G. L. Stephens, 2004: Information content of infrared satellite sounding measurements with respect to CO$_2$. *J. Appl. Meteo.*, **43**, 373–378.

Engelen, R. J., G. L. Stephens, and A. S. Denning, 2001b: The effect of co$_2$ variability on the retrieval of atmospheric temperatures. *Geophys. Res. Let.*, **28**, 3259–3262.

Enting, I. G., C. M. Trudinger, and R. J. Francey, 1995: A synthesis inversion of the concentration and *d*13C of atmospheric CO$_2$. *Tellus, Ser. B*, **47**, 35–52.

Fan, S.-M., M. Gloor, J. Mahlman, S. Pacala, J. Sarmiento, T. Takahashi, and P. Tans, 1998: A large terrestrial carbon sink in North America implied by atmospheric data and oceanic carbon dioxide data and models. *Science*, **282**, 442–446.

GLOBALVIEW-CO$_2$, 2003: Cooperative Atmospheric Data Integration Project - Carbon Dioxide. CD-ROM, NOAA CMDL, Boulder, Colorado [Also available on Internet via anonymous FTP to ftp.cmdl.noaa.gov, Path: ccg/co2/GLOBALVIEW].

Gurney, K. R., R. M. Law, A. S. Denning, P. J. Rayner, D. Baker, P. Bousquet, L. Bruhwiler, Y.-H. Chen, P. Ciais, S. Fan, I. Y. Fung, M. Gloor, M. Heimann, K. Higuchi, J. John, T. Maki, S. Maksyutov, K. Masarie, P. Peylin, M. Prather, B. C. Pak, J. Randerson, J. Sarmiento, S. Taguchi, T. Takahashi, and C.-W. Yuen, 2002: Towards robust regional estimates of CO$_2$ sources and sinks using atmospheric transport models. *Nature*, **415**, 626–630.

Harris, B. A. and G. Kelly, 2001: A satellite radiance-bias correction scheme for data assimilation. *Q. J. R. Met. Soc.*, **127**, 1453–1468.

Kaminski, T., M. Heimann, and R. Giering, 1999: A coarse grid three-dimensional global inverse model of the atmospheric transport, 2, Inversion of the transport of CO$_2$ in the 1980s. *J. Geophys. Res.*, **104**, 18555–18581.

Lorenc, A. C., 1986: Analysis methods for numerical weather prediction. *Q. J. R. Met. Soc.*, **112**, 1177–1194.

Matricardi, M., 2003: RTIASI-4, a new version of the ECMWF fast radiative transfer model for the infrared atmospheric sounding interferometer. Technical Memoranda, 425, ECMWF.

Matricardi, M., F. Chevallier, G. Kelly, and J.-N. Thépaut, 2004: An improved general fast radiative transfer model for the assimilation of radiance observations. *Q. J. R. Met. Soc.*, **130**.

McNally, A. P. and P. D. Watts, 2003: A cloud detection algorithm for high-spectral-resolution infrared sounders. *Q. J. R. Met. Soc.*, **129**.

O'Brien, D. M. and P. J. Rayner, 2002: Global observations of the carbon budget 2. CO$_2$ column from differential absorption of reflected sunlight in the 1.61 μm band of CO$_2$. *J. Geophys. Res.*, **107**(D18).

Peylin, P., P. Bousquet, P. Ciais, and P. Monfray, 2000: Differences in CO$_2$ flux estimates based on a time-independent versus a time-dependent inversion method. In: P. Kasibhatla et al., ed., *Inverse Methods in Global Biogeochemical Cycles, Geophys. Monogr. Ser.,* vol. 114, pp. 811–841. AGU, Washington, D. C.

Rayner, P., I. Enting, R. Francey, and R. Langenfelds, 1999: Reconstructing the recent carbon cycle from atmospheric CO$_2$, d13C, and O$_2$/N$_2$ observations. *Tellus, Ser. B*, **51**, 213–232.

Rayner, P. and D. O'Brien, 2001: The utility of remotely sensed CO$_2$ concentration data in surface source inversions. *Geophys. Res. Let.*, **28**, 175–178.

Rodgers, C. D., 2000: *Inverse Methods for Atmospheric Sounding. Theory and Practice*. World Sci., River Edge, N. J.

Rumelhart, D. E., G. E. Hinton, and R. J. Williams, 1986: Learning internal representations by error propagation. In: D. E. Rumelhart and McClelland, eds., *Parallel distributed processing: Explorations in the macrostructure of cognition 1*, pp. 318–362. MIT Press.